Feedback loops in star formation: The interplay between Waterloo 01 and Sh 2-208

[1]Harmeen Kaur (ARIES, Nainital,India)
[2]Saurabh Sharma (ARIES Nainital, India)
[3]Lokesh Dewangan (PRL, Ahmedabad, India)
[4]Devendra Ojha (TIFR, Mumbai, India)
[5]Alok Durgapal (Department of Physics, Kumaun University, Nainital, India)
[1]harmeenkaur.kaur229@gmail.com

Star Formation, Stellar Feedback and Ecology of Galaxies, Visegrad, Hungary, from 26th- 30th May 2025.

OBJECTIVE

In this study we performed multi-wavelength analysis of two regions Waterloo 01 and Sh 2 -208 located at the ineter arm island between Cygnus and Perseus arm. We calculated physical parameters such as, physical structure, age distance, mass function, and mass segregation. We also discussed about the positive impact of massive star(s) on the surroundings of Waterloo 01 cluster and possible Hub-filament system Sh 2-208.

INTRODUCTION

Young star clusters are idiosyncratic for astrophysical research (*Portegies Zwart et al. 2010; Adamo et al. 2020*). Star clusters are formed by the gravitational collapse of dense regions within molecular clouds, where gas and dust accumulate. As these regions collapse under their gravity, they fragment into smaller clumps, each potentially forming a star (*Lada & Lada 2003; Krumholz et al. 2019*). When a cluster of stars forms, particularly massive stars, they emit intense ultraviolet radiation that ionizes the surrounding hydrogen gas, creating HII regions, large ionized areas of hydrogen (*Krause et al. 2020*). Massive stars ($M_\odot \geq 8$) play a crucial role in forming new generations of stars and star clusters (*Walch 2014*). Their strong stellar winds and radiation pressure can compress nearby gas and dust, leading to further collapse and generating a low-density bubble that expands over time (*McKee et al. 1984; van Marle et al. 2015)*. This star formation cycle and feedback from massive stars are fundamental to the evolution of galaxies and the continuous generation of star clusters.

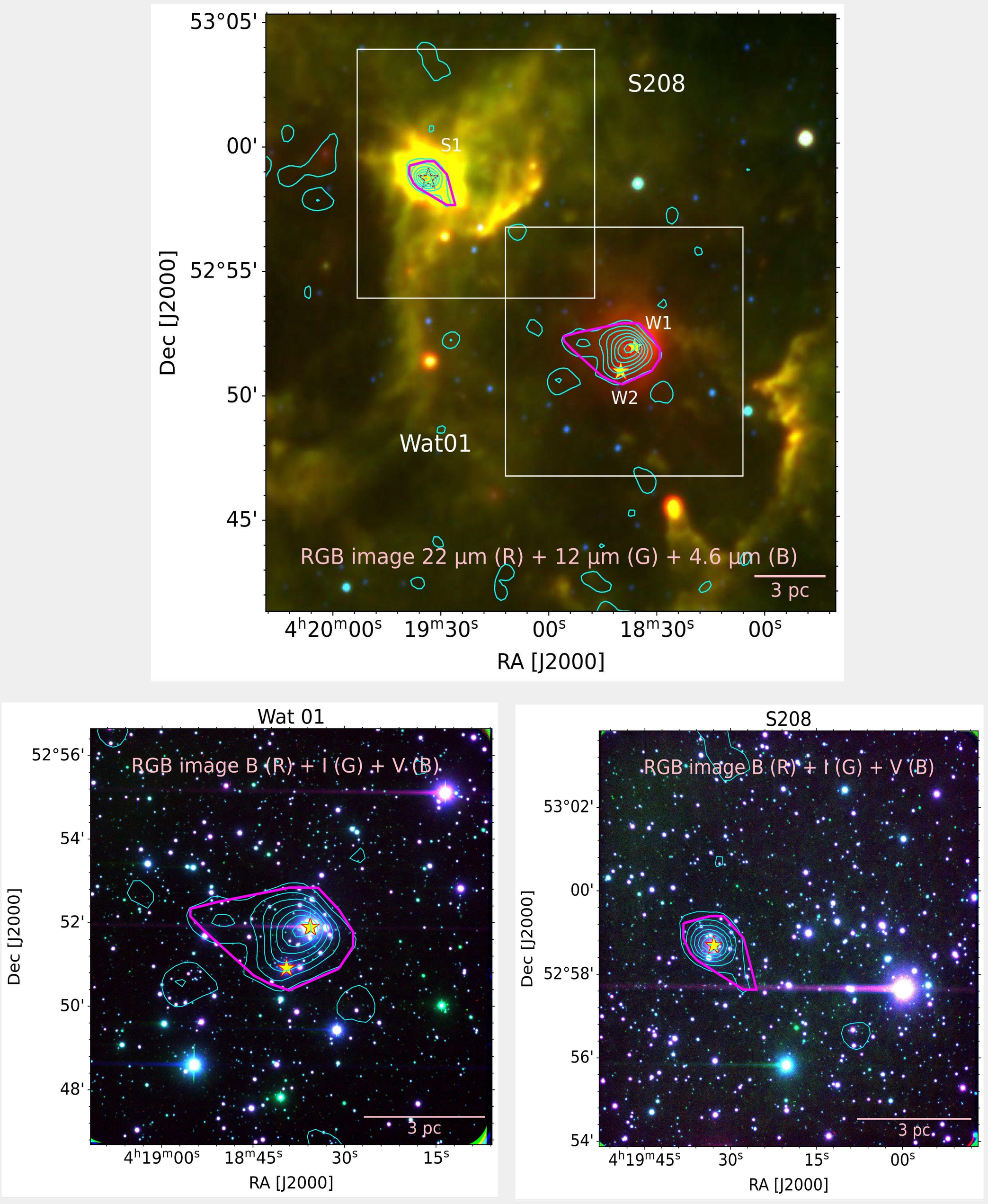

Figure 1: Upper panel: Color-composite image of the 24′ × 24′ FOV of the star forming region Sh2-208 embracing Wat01 cluster. This color image is overlaid with isodensity contours generated from the NIR catalog (2MASS+UKIDSS). The lowest level for the isodensity contours is 2σ above the mean stellar density (i.e., 18 stars arcmin^{-2}) with a step size of 1σ (3.5 stars arcmin^{-2}). White boxes delineate the optically observed 10 × 10 arcmin^2 FOV from 2m HCT, Hanle, and magenta curves are the convex hell for the lowest density contour for both regions. Yellow asterisk symbols depict the location of massive stars in both regions. Lower panels: Color-composite image for Wat01 (Left) and S208(Right). Overlaid contours and convex hull are the same as an upper panel.

DATA REDUCTION

The broadband U BV (RI)c optical photometric data of the Wat01 centered at α_{J2000}: 04h18m38.728s, δ_{J2000}: +52°51′40.24″; l = 151°.272 and b° = 1.789, and S208 centered at α_{J2000}: 04h19m19.76s, δJ_{2000}: +52° 58′50″; l = 151°.262 and b° = 1.95, were acquired by using the 2048 × 4096 pixel^2 Hanle faint object spectrograph camera (HFOSC) mounted at 2-m Himalayan Chandra Telescope (HCT), Hanle, Ladakh, India. The entire chip (Plate scale: 0.296 arcsec/pixel) covers a ~ 10′ × 10′ FOV on the sky. The observations were carried out in the binning mode of 2×2 pixels to improve the signal-to-noise ratio (SNR). The read-out noise and gain of the CCD are 4.8 e− and 1.22 e−/ADU respectively. The broad-band U,B,V,(RI)c observations of Wat01 and S208 were standardized by observing standard stars in the SA98 Landolt field (*Landolt 1992*) centered at αJ2000: 06h52m12s, δJ2000: -00◦19′17″. Many bias and flat frames were also taken during observations. Several short and deep (long) exposure frames were taken to observe both bright and faint stars in the field. The basic data reduction, including image cleaning, photometry, and astrometry, was done using the standard procedure explained in *Sharma et al. (2020)*; *Pandey et al. (2020)*; *Kaur et al. (2020)*. Calibration of the instrumental magnitudes to the standard system was done by using the procedures outlined by *Stetson (1992).* The calibration equations derived by the least-squares linear regression are as follows:

$$u = U + (3.096 \pm 0.027) - (0.009 \pm 0.017)(U - B) + (0.338 \pm 0.037)X_U$$

$$b = B + (1.023 \pm 0.012) - (0.001 \pm 0.005)(B - V) + (0.181 \pm 0.018)X_B$$

$$v = V + (0.626 \pm 0.004) - (0.085 \pm 0.007)(R - I_c) + (0.010 \pm 0.006)X_V,$$

$$r_c = R_c + (0.563 \pm 0.009) - (0.003 \pm 0.004)(V - R_c) + (0.045 \pm 0.013)X_R,$$

$$i_c = I_c + (0.831 \pm 0.006) - (0.065 \pm 0.009)(R - I_c) + (0.037 \pm 0.008)X_I$$

where U, B, V, R_c, and I_c are the standard magnitudes; u , b , v, r_c , and i_c are the instrumental aperture magnitudes normalized per second of exposure time; and X's is the air mass in respective bands. The V and I_c band detection limits (photometric error< 0.1 mag) for our observations are found to be 21.75 mag and 21.88 mag, respectively, for Wat01, and 21.19 mag and 21.47 mag, respectively, for S208. The astrometry of stars were done by using the Graphical Astronomy and Image Analysis (Gaia) Tool with rms noise of the order of ~ 0″.3

STRUCTURAL PARAMETERS

Structural Parameters using Iso-density contours analysis:

Cluster	n_{total}	n_{hull}	A_{hull} ($'^2$)	$A_{cluster}$ ($'^2$)	$R_{cluster}$ ($'$)	R_{circ} ($'$)	Aspect ratio
Wat01	209	13	6.53	6.97	1.49	2.08	1.95
S208	69	9	2.04	2.34	0.86	1.25	2.11

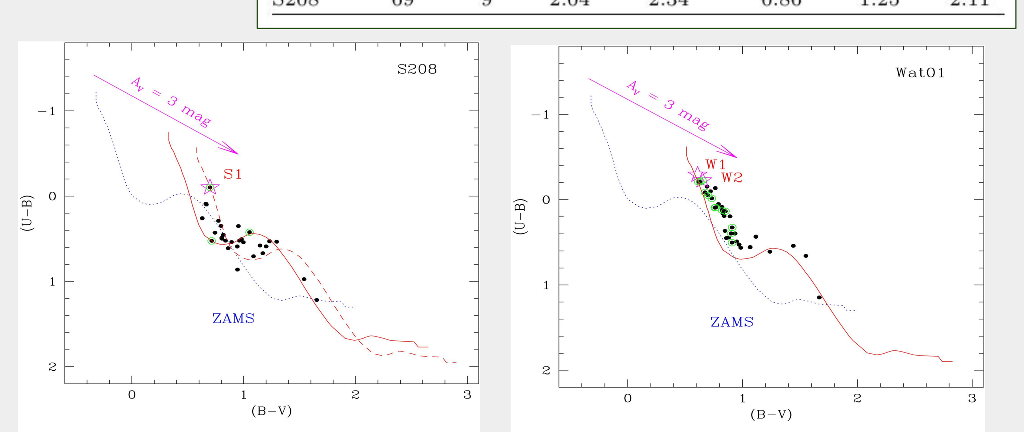

Figure 2: Right:(U − B) vs.(B − V) TCDs for stellar sources within hull of Wat01 cluster region. The blue curve denotes the intrinsic ZAMS for Z = 0.02 by *Pecaut & Mamajek (2013),* shifted along the reddening vector for E(B − V) = 0.83 mag (red continuous curve). Cluster members (Pμ >80%) are highlighted by green open circles, and magenta asterisk symbols are the location of massive OB-type stars. Left: Same as left panel but for the S208 cluster region with reddening value E(B − V) = 0.65 mag.

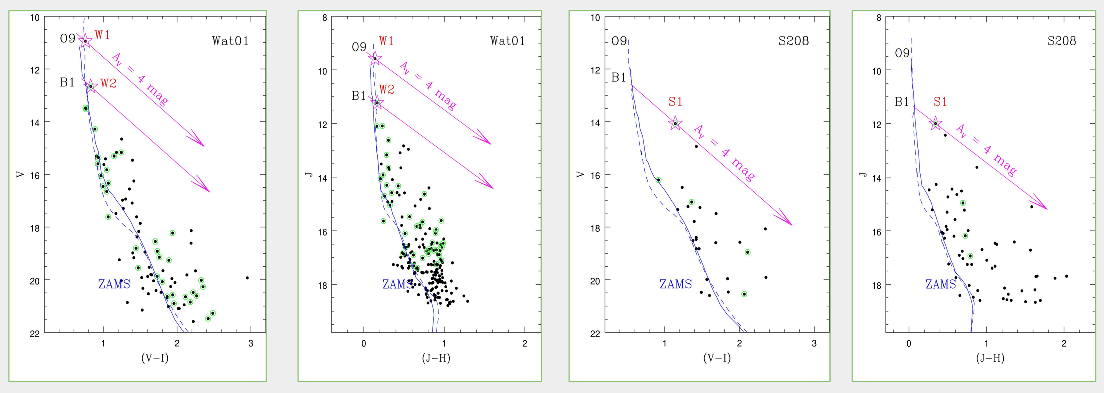

Figure 3: Optical (V vs. (V − I)) and NIR (J vs. (J − H)) color-magnitude diagrams for Wat01 and S208 cluster regions. Continuous and dotted blue curves represent the Zero Age Main Sequence (ZAMS) of *Pastorelli et al. (2019)* and *Pecaut & Mamajek (2013)* respectively, corrected for the distance of 3.53 kpc and reddening value of E(B − V) = 0.83 mag for Wat01 and E(B − V) = 0.65 mag for S208 regions. Green open circles are the identified member stars from proper motion analysis, whereas magenta asterisk symbols are the location of massive OB-type stars in the respective clusters. Reddening vectors along the massive stars are represented by magenta arrows for A_V = 4 mag in each cluster region.

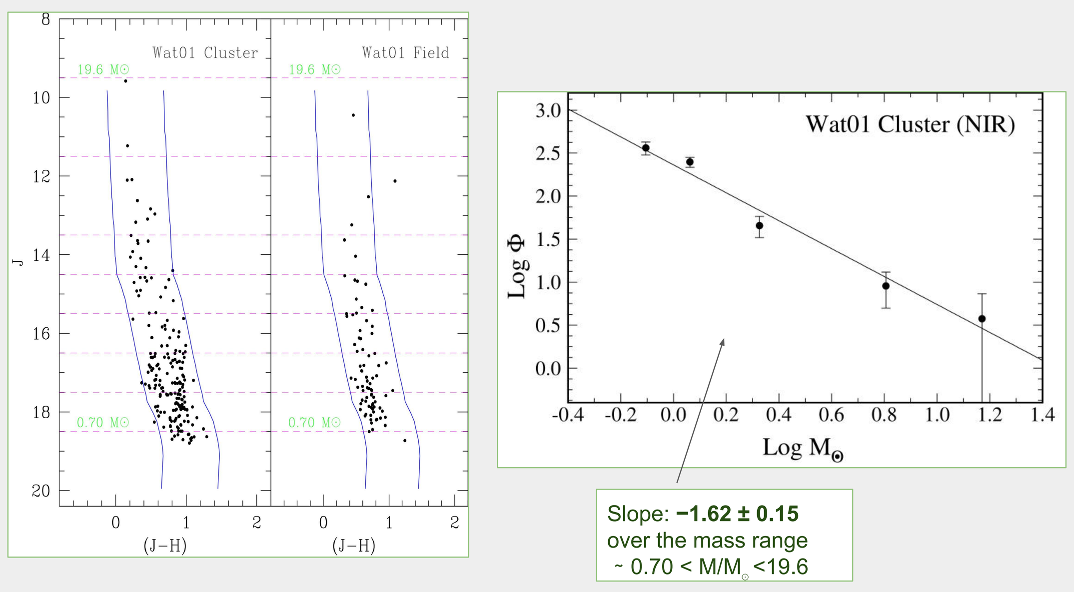

Figure 4: Left panel: J versus (J − H) CMD for (a) stars within the cluster region, (b) stars within the field region of the same area as of cluster. The curves represents envelop of +0.6 mag (right curve; A_v = 4.62 mag) and -0.2 mag (left curve; A_v = 1.33 mag) on the CMD from the isochrone of *Pecaut & Mamajek (2013)*. Left panel: A plot of the mass function (MF) for the Wat01 region using the NIR (2MASS+UKIDSS) data. Logϕ represents log(N/d log m), and the error bars represent standard ±√N errors. The solid line shows a least squares fit to the MF distribution.

LARGE SCALE ENVIRONMENT

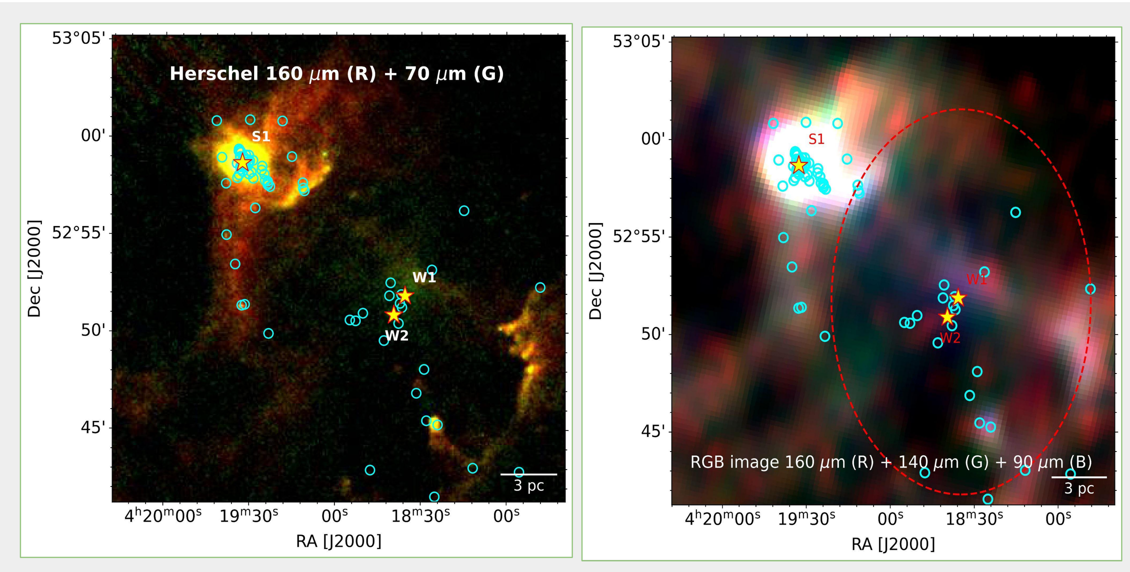

Figure 5: Left panel: 24′ × 24′ area around Wat01 and S208 regions is shown by color-composite image procured from Herschel 160 µm, Herschel 70 µm . Right panel: Color image obtained by AKARI 160µm (red), AKARI 140µm (green) and AKARI 90µm (blue) are used to create color image of region enclosing wat01 and S208 region. The red-dotted region represents the ring/bubble-like structure around the Wat01 region. The cyan circles and red asterisk symbols are the locations of young stellar objects (YSOs) and massive stars, respectively, in all panels.

MOLECULAR MORPHOLOGY

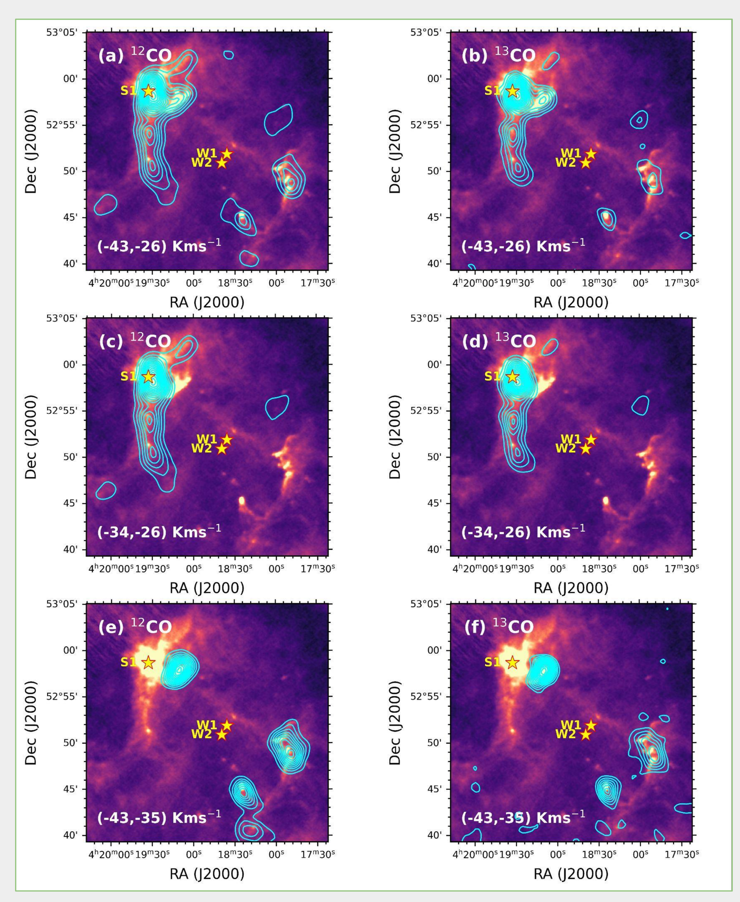

Figure 6: Herschel 160µm images overlaid with 12CO (J = 1 − 0) and 13CO (J = 1 − 0) emission contours at different velocities..

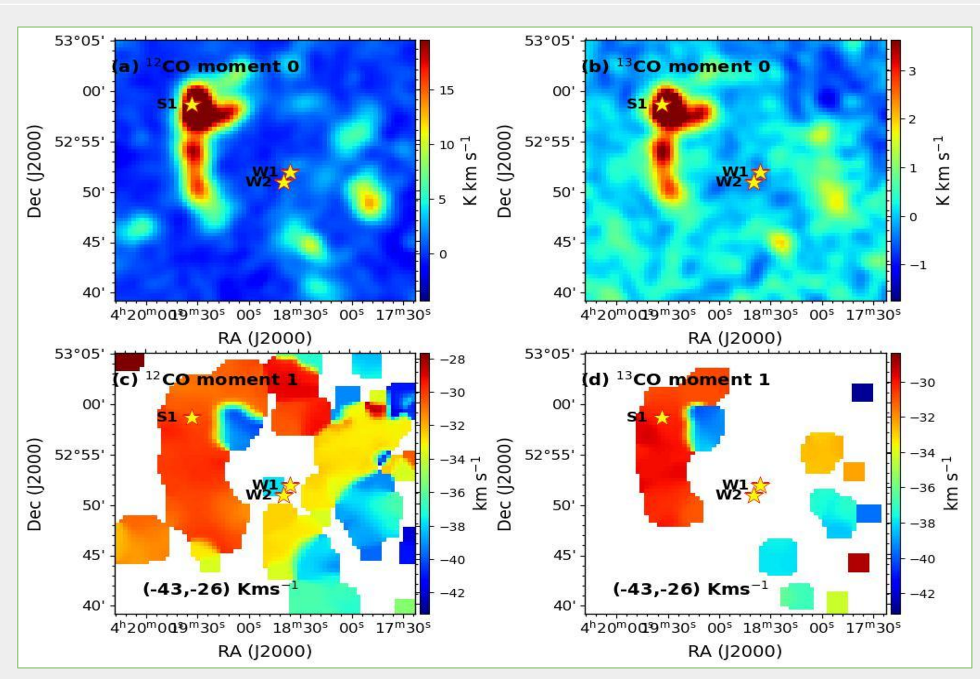

Figure 7: Left panel represent the moment-0 map (Integrated intensity) and moment-1 map (Intensity-weighted velocity), collapsed images for the 12 CO(J = 1 − 0) cube of 24′ × 24′ region around the Wat01 and S208 regions. The right panel represents the same for 13 CO(J = 1 − 0) cube of the same area. The asterisk symbols mark the location of massive stars in the regions.

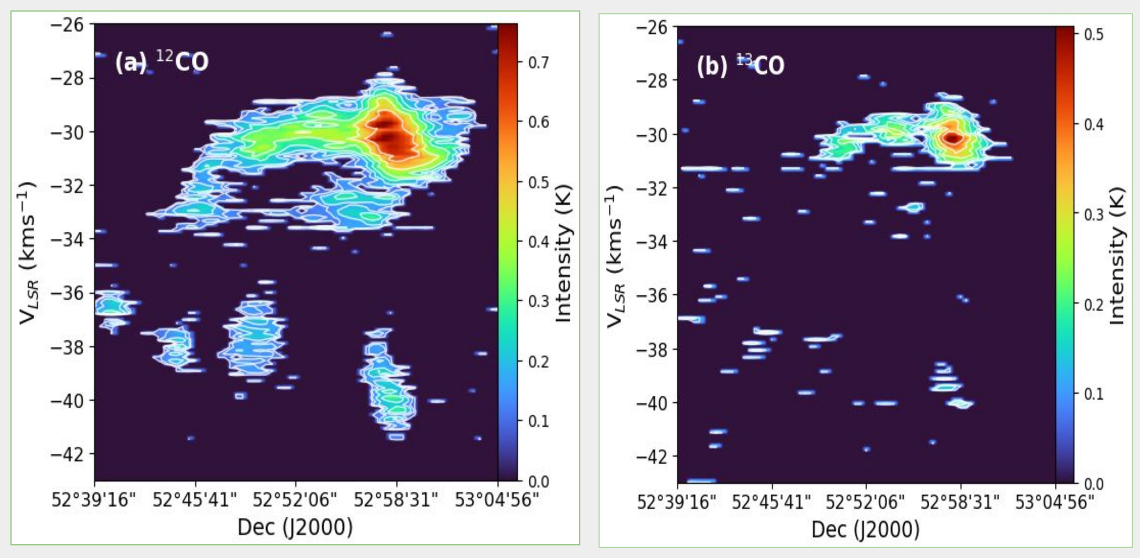

Figure 8: The 12CO(1 − 0) and 13CO(1 − 0) position-velocity diagram of the velocity as a function of declination (δ).

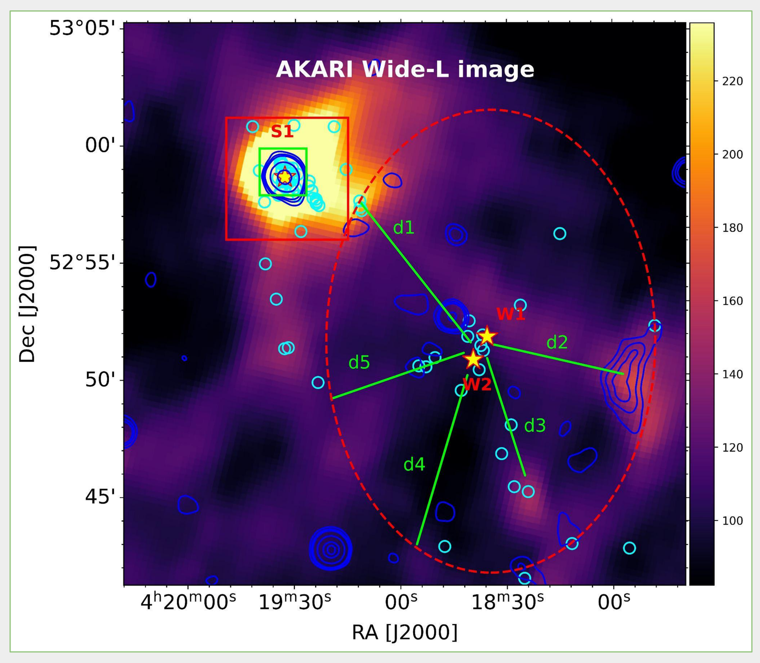

Projected D_s	D_s (pc)	P_{HII} (dynes cm^{-2})	P_{rad} (dynes cm^{-2})	P_{wind} (dynes cm^{-2})	P_{total} (dynes cm^{-2})
d1	7.8	1.33×10^{-11}	1.32×10^{-12}	1.26×10^{-14}	1.46×10^{-11}
d2	5.8	2.07×10^{-11}	2.39×10^{-12}	2.28×10^{-14}	2.31×10^{-11}
d3	5.4	2.31×10^{-11}	2.76×10^{-12}	2.63×10^{-14}	2.59×10^{-11}
d4	7.7	1.35×10^{-11}	1.36×10^{-12}	1.29×10^{-14}	1.49×10^{-11}
d5	6.1	1.92×10^{-11}	2.16×10^{-12}	2.06×10^{-14}	1.97×10^{-11}

Figure 9: The AKARI Wide-L image of 24′ × 24′ area around Wat01 and S208 regions. The yellow asterisk symbol and cyan circles represent the massive stars and YSOs in the regions. The red dotted ring shows the bubble/ring-like feature around the Wat01 region. The d1, d2, d3, d4, and d5 are various projected distances along the bubble for which total pressure from massive stars 'W1' and 'W2' has been calculated. The blue contours mark the 1.4 GHz NVSS radio continuum emission in and around the clusters. The lowest NVSS contour is 1.35 mJy/beam with a 0.9 mJy/beam step size. The red box shows the area for which Spitzer data is available and green box is the zoomed-in view of S208 region.

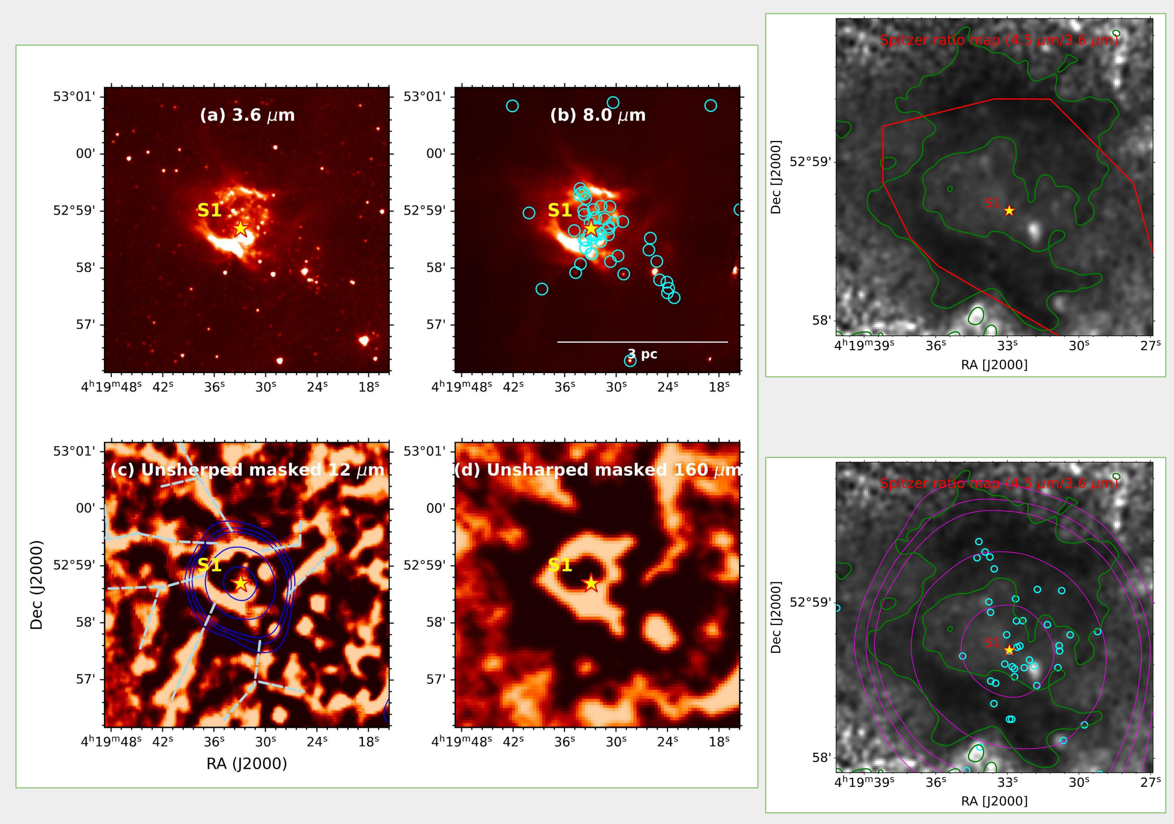

Figure 10: The Zoomed-in (cf; red box in figure 10) multi-wavelength picture of the S208 region ranging from NIR to FIR. Blue curves show the NVSS 1.4 GHz contours. The lowest NVSS contour is 1.35 mJy/beam with a 0.9 mJy/beam step size. The yellow asterisk symbol shows the location of the massive star 'S1'. The cyan circles show the distribution of identified YSOs. In the upper right panel: red curve represents the hull area of the infrared cluster [BDS2003]64, and in lower left panel magenta contours are the NVSS 1.4 GHz contours with cyan circled as identified YSOs.

CONCLUSIONS

- ★ We determined the structural parameters of the Wat01 and S208 clusters through iso-density contour analysis employing the NN method. Our findings indicate these clusters have elongated morphology (aspect ratio ~ 1.95 for Wat01 and ~ 2.11 for S208). The corresponding circular radii for Wat01 and S208 are measured as ~ 1.53 pc and ~ 0.88 pc, respectively.
- ★ Using Gaia DR3 proper motion data, we have identified 52 stars as the most probable cluster members of the Wat01 cluster. As estimated from the Gaia parallax and isochrone fitting method, the distance of both clusters is estimated as ~ 3.53±0.55 kpc. The reddening towards the Wat01 cluster is estimated to be E(B − V) ~ 0.83 mag, while for the S208 cluster region, it is E(B − V) ~ 0.65.
- ★ By using deep NIR data, we also derived the MF slope (Γ) in the Wat01 cluster region as 1.62±0.15 within the mass range $\sim 0.7 < M/M_\odot < 19.6$. This slope is steeper than the Salpeter value (−1.35). This indicates an excess number of low-mass stars in the cluster. The Wat01 cluster also shows the effect of mass segregation, whereas the dynamical age (~ 11.4 − 18.75 Myr) of this cluster is more than the upper age of this cluster (~ 8.1 Myr). This indicates that the massive stars have formed in the inner region of the Wat01 cluster
- ★ The MIR emission and distribution of PDR in the region indicates a bubble/ring-like feature of warm gas around the Wat01 cluster/massive stars. The location of massive stars also coincides with the peak of the radio continuum emission. Towards the southwest of the massive stars, we can see IBL regions and globules pointing towards the massive stars. While towards the northeast of massive stars, the S208 cluster is located at the bubble's boundary. This morphology resembles the expanding H ii region. The total pressure value (~ 10−10 dynes cm−2) from massive stars at various projected distances is sufficient enough to influence star formation in their surrounding molecular clouds.
- ★ We studied molecular cloud morphology/dynamics in this region by using the high resolution 12CO (J = 1 − 0) and 13CO (J = 1 − 0) molecular maps. These velocity-resolved observations show the characteristic kinematics of a shell expanding toward us: at low velocities (~ −38 kms^{-1}), the emission is centralized as well as along the inner rim of the bubble, and as the velocity increases, a ring/bubble-shaped structure emerges and increases in radius until the velocity of ~ −30 kms^{-1} is reached. The red-shifted emission indicates expansion with a velocity of ~ 8 kms^{-1} away from us with respect to the velocity of the cloud associated with the Wat01 region. The overall structure of this region strongly suggests an interaction between a massive star and a bubble moving in relation to the surrounding gas.

REFERENCES

- Portegies Zwart, S. F., McMillan, S. L. W., & Gieles, M. 2010, ARA&A, 48, 431.
- Adamo, A., Zeidler, P., Kruijssen, J. M. D., et al. 2020, SSRv, 216, 69.
- Lada, C. J., & Lada, E. A. 2003, ARA&A, 41, 57.
- Krumholz, M. R., McKee, C. F., & Bland-Hawthorn, J. 2019, ARA&A, 57, 227.
- Krause, M. G. H., Offner, S. S. R., Charbonnel, C., et al. 2020, SSRv, 216, 64.
- Walch, S. K. 2014, in Astrophysics and Space Science Proceedings, Vol. 36, The Labyrinth of Star Formation, ed. D. Stamatellos, S. Goodwin, & D. Ward-Thompson, 173.
- McKee, C. F., van Buren, D., & Lazareff, B. 1984, ApJL, 278, L115.
- Van Marle, A. J., Meliani, Z., & Marcowith, A. 2015, A&A, 584, A49.
- Pecaut, M. J., & Mamajek, E. E. 2013, ApJS, 208, 9.
- Pastorelli, G., Marigo, P., Girardi, L., et al. 2019, MNRAS, 485, 5666.
- Sharma, S., Ghosh, A., Ojha, D. K., et al. 2020, MNRAS, 498, 2309.
- Kaur, H., Sharma, S., Durgapal, A., et al. 2023, Journal of Astrophysics and Astronomy, 44, 66.
- Kaur, H., Sharma, S., Dewangan, L. K., et al. 2020, ApJ, 896, 29.
- Pandey, A. K., Upadhyay, K., Nakada, Y., & Ogura, K. 2003, A&A, 397, 191,